Optimal Power Quality Enhancement using a Radial Distribution System with an Improved Unified Power Quality Conditioner

OLUWAFUNSO OLUWOLE OSALONI[1], AYODEJI STEPHEN AKINYEMI[2],
ABAYOMI ADURAGBA ADEBIYI[2], KATLEHO MOLOI[2], AYODEJI OLALEKAN SALAU[1,3]
[1]Department Electrical Electronic and Computer Engineering,
Afe Babalola University, Ado Ekiti, Ekiti-State,
NIGERIA

[2]Department Electrical Power Engineering,
Durban University of Technology, Durban,
SOUTH AFRICA

[3]Saveetha School of Engineering,
Saveetha Institute of Medical and Technical Sciences,
INDIA

Abstract: - Massive electric power distribution over long distances with consequential Power Quality (PQ) challenges such as voltage sags and power losses are some of the significant attributes of a Radial Distribution Network (RDN). Deployment of Power Angle Regulated (PAR) based Unified Power Quality Conditioner (UPQC) in a distribution network is also securing attraction because of the latest recorded achievements and improvements in Voltage Source Inverter (VSI) built power electronic systems. However, optimal allocation of this kind of device to mitigate PQ problems remains a challenge for achieving set objectives. Consequently, this study considers the best possible allocation of PAR and Improved-UPQC know as I-UPQC in the distribution network to enhance power network performance. The identification of optimal location is achieved through the application of hybridization of the Genetic Algorithm and Improved Particle Swarm Optimization (GA & IPSO). The deterministic approach is based on the weight factor of various objective functions. The allocation is attained with a selection of reactive power control between inverter connected in parallel and series and control angle variables of the device through its dynamic involvement of total system loss derivatives. Performances of the I-UPQC based distribution system during diverse power transfers are observed. Convergence characteristic of deterministic approach at different disturbance percentages is analyzed and presented. Imaginary power circulation enhanced the voltage-associated challenges at the range of 0.949 to 0.9977. Hence, power dissipation minimized to 1.15 percent compared to the initial 3.35 percent, according to results of I-UPQC allocation in RDN utilizing mathematical and optimization technique. Additionally, the network losses, voltage dip, and minimum bus voltage profile all fall within the regulatory standards of less than 2%, 5%, and 5%, correspondingly. Also, the performance of the compensated network for both ordinary and optimized scenarios indicated the fitness of the projected method in accomplishing an operational optimization of RDN, specifically for voltage profile (VP) improvement and I-UPQC's series and shunt inverter share imaginary power.

Key-Words: - Power Quality, Unified Power Quality Conditioner, Power Angle Control, Particle Swarm Optimization, Genetic Algorithm.

Received: August 19, 2022. Revised: August 16, 2023. Accepted: September 13, 2023. Published: October 9, 2023.

1 Introduction

The deficiency of imaginary power in grids results in variability, which triggers voltage drop and oscillation. Ameliorating imaginary power at an optimal point would eliminate voltage instability problems and substantially enhance the grid reaction. Man-aging imaginary power is considered compensation, while the compensator installation is usually placed where there are imaginary loads. Many authors have come up with re-active power compensation and sag/swell mitigation in recent times. Presentation of tap changing transformer which is used to control imaginary power in, [1], but

because of transformer tap has a low range limits its application (can result in voltage swings). Optimal capacitor placement is determined in, [2], [3], and this is achieved using a heuristic search-based approach. Due to factors like controlling existing ameliorators and the financial costs of removing some absorbing loads, this method has gained less support than the hypothetical power injection option, which would make its shortcomings far more obvious. The task was completed in, [2], where a cuckoo search-based approach had been used to distribute static shunt capacitors in the RDN. The process of putting in a constant and changeable regulating capacitive load has been used in, [4]. The hypothetical energy provided by the shunt capacitors described in, [4], has an extremely poor response time for unexpected varying loads.

In, [5], a fuzzy concept-based optimization method is used to allocate multi-objective capacitors in distribution systems. Furthermore, another power quality device is a flexible AC transmission system (FACT), but they find their application in optimal imaginary power amelioration in the LV distribution network. A distribution static compensator (DSTATCOM), for example, is an extremely costly FACTs device, [6]. The com-bination of VSI connected in series and parallel connected with DC-link back-to-back is considered as a general solution for imaginary power compensation, which is named UPQC, are utilized. Additionally, UPQC became a multi-dimensional FACT technology due to its capacity to correct for a variety of PQ-related factors, including voltage dips, overvoltage, imbalance voltage, imaginary current, flashes, and distortions, [7]. By injecting a monitored and adjustable quadrature voltage simultaneously to address under-voltage difficulties, the VSI linked in series can produce real power and imaginary power, [8]. The work done in [9] present a comparative analysis of models of UPQC.

However, the series VSI connected in series can concurrently produce imaginary and real power, as shown in, [10]. In most of the articles on UPQC, it can be observed that it is either protecting a single load or connected to two bus systems that contain mostly non-linear or sensitive loads. Considering the possibility of the presence of this type of load in RDN and the level of sensitivity required for its protection, there is a need for the proper allocation of I-UPQC in the larger network. I-UPQC can produce imaginary power amelioration in a distribution network, [11]. The use of such a method enables the de-termination of the assignment optimizing ameliorator, in which all grid variables seem to be in their ideal state. In, [12], imaginary power amelioration is performed with PAC in this work, and amelioration without including microgrids is performed. This allows for enhancement on, [13], by taking into account DG supply, which is a crucial tendency to use due to various consumer preferences. Electricity issues like those seen in DGs studies will unquestionably be impacted by the introduction of loads that utilize fictitious energy in operational systems. As a result, [14], proposes an ideal strategy that implements the simultaneous deployment of DGs with dormant advanced metering systems. Owing to the ability of DGs to turn passive network to active network it was treated in but on the contrary using DG with UPQC is not mentioned. However, due to the clean nature of renewable energy, no cost of fuel, its integration into RDN through PAC of UPQC re-quired more attention.

The goal of this research is to investigate the best apportionment to modify the I-UPQC architecture compared to ordinary UPQC in the RDN in such a way as to strengthen the PQ in the power system. The contribution of the article includes the following:

- Development of proper application of GE-IPSO in RDN
- Reactive power-sharing with the utilization of both inverters of I-UPQC simultaneously in two bus networks analytically
- Optimal PQ enhancement through the impact of DG interconnection through I-UPQC on network power dissipation and voltage dip/surge using photovoltaic DG in an RDN network.

2 Basic I-UPQC Modelling

Figure 1 shows the practical block diagram of UPQC, an integrated optimizer of PQ centered on PAC which is employed in this study and incorporates two series & shunt inverters. The series inverter is utilized to reduce supply voltage dip. Additionally, shunt inverters are employed for correction when harmonics and the imaginary element of the load current are present. As indicated in Figure 2a and Figure 2b, series voltage (V_{Se}) and shunt compensatory current (I_{Sh}) would be injected by respective series inverter and shunt inverter under normal and dip voltage conditions. The series inverter injects electricity under convectional operational requirements in the UPQC-PAC design.

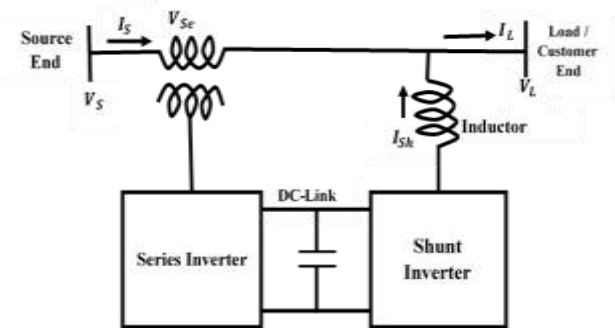

Fig. 1: Basic block diagram of UPQC, [11]

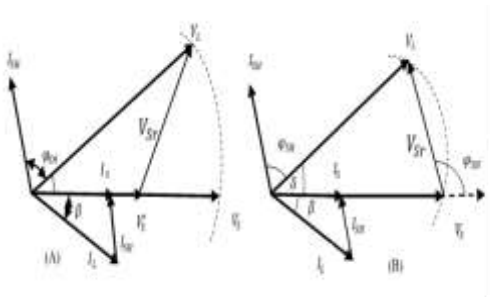

Fig. 2: Evaluation of shunt and series amelioration (a) under a voltage dip (b) at optimum conditions

2.1 Multi-Objective Planning Concept

This study presents detailed development of a multi-objective framework that identifies the best site for I-UPQC, the best value for ameliorating imaginary output at the preferred destination, and the best amount of k_{Sinj}. To concurrently identify the optimal variable, three objectives are minimized. They comprise, [15]:

First Goal 1: Rating of I-UPQC (VA)

Goal 1: $S_{I-UPQC} = S_{Sh} + S_{Se}$

S_{I-UPQC} denotes the objective function. such that S_{Sh}, S_{Se} represent the apparent powers of series and shunt VSI, respectively.

Second Goal 2: RDN power loss

Goal 2: $P_{Loss}^{I-UPQC} = \sum_{jk\epsilon\gamma}\{I_L(mn)\}^2.r(mn)$

such that, $I_L(mn)$, $r(mn)$ represents the branch mn line current and resistance and set γ comprise of all branches in a network.

Third Goal 3: Degree of nodes with under voltage problem (DNUVP)

Goal 3: DNUVP = $100\left(\frac{N_{I-UPQC}^{UV}}{N_{Base}^{UV}}\right)$

The number of the bus with under-voltage with I-UPQC is denoted with N_{I-UPQC}^{UV}, and N_{Base}^{UV} indicate the number of bus haven under-voltage without I-UPQC.

2.2 Genetically Modifies Particle Swarm Optimization

GA-IPSO is a variety of PS that genetically modifies to optimally solve multi-objective problems in which equivalent Fitness Function (FF) are attached to the particles. The state-of-art literature review in, [16], [17], [18], show many PSO variations. The Pareto-dominance method populates most of the optimization strategies. The actual goals of each of these methods are to find a set of Non-Dominated Results (NDR) that is closer to the set of pareto-optimal solutions (superior convergence) and to guarantee minimal global convergence as opposed to regular PSO. Hence, with selection properly guided by each particle, better convergence can be achieved. For this GA-IPSO, two variants were used, which include PSO and GA. The behavior of the non-dominated sorted genetic algorithm stimulated the PSO, [19]. PSO uses the population of individuals from the most recent iteration and the one before it to identify non-dominated solutions. So, the Pareto optimal solutions are sorted using a niche technique. The PSO, on the other hand, is built on a collection of elite archived NDS developed by optimization algorithms and is applied to distribute fitness to each member of the archive while the present population is evolving. According to the PSO's global optimal (gbest) architecture, the IPSO particle guide selection process is carried out, [20], [21].

Begin

//η_{pop} =size of IPSO population

//η_{gen} =Highest amount of iterations

Produce preliminary population for IPSO at random by means of the encoding system.

Evaluation of the objective functions and explanation of the particle;

Find the first, undominated resolution.*;*

Learn the basic guideline;

Repetition=1;

While *repetition*<=//η_{gen}

For i=*1,……,*η_{pop}

Choose a guide from the list of rules to attach to particle i,

Modify this same particle's speed and location;

Get the location and parameters for I-UPQC by decoding the particle;

Incorporate the I-UPQC concept through power flow;

End for

Determine the *non-dominant solutions;*

Discover the new set of instructions;
Repetition =repetition+1;

End while

Optimal solutions comprise the ultimate group of non-dominated options.

location, size, and the parameters for I-UPQC,

End.

Pseudocodes for the scheduling of fictitious power amelioration utilizing I-UPQC allocation and GA-IPSO are shown in Figure 3.

2.3 Planning Algorithm

The IPSO comprises two major provision subprogrammes, i.e., particle encrypting/decrypting structure and power flow with the I-UPQC model. Three significant segments consist of 1) I-UPQC allocation in the system, 2) the quantity of imaginary power amelioration demand, and 3) k_{Sinj} are parts of GA-IPSO particle coding. The first set of segments of the particle is always transformed to its closet digit during decoding. The solution that violates the last constraint is set aside. The pseudocodes for the comprehensive arrangement algorithm are displayed in Figure 3.

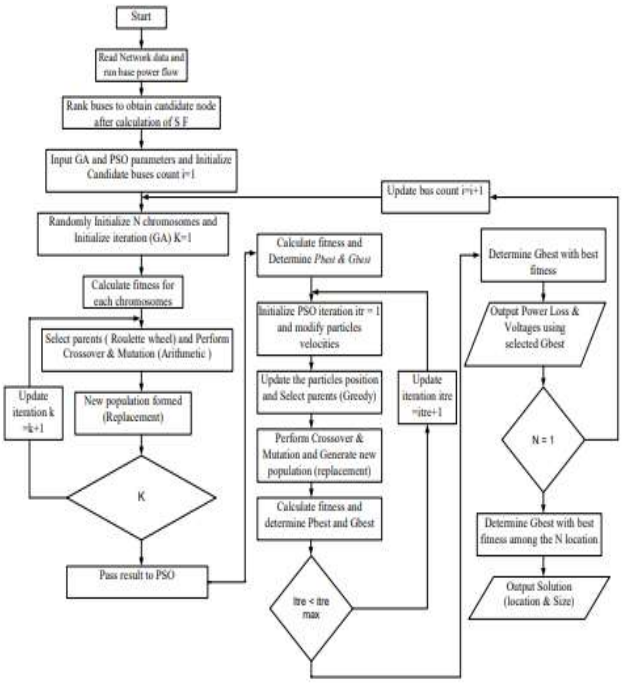

Fig. 3: Algorithms flow diagram for GA-IPSO, [21]

3 Network Parameters for the RDN 33-bus and 69-bus

The network of 33-bus standard IEEE test system implementation framework is presented in this segment, with 3.69 MW and 2.3 MVAR, 5 ties, and 68 sectionalizing lines that separate the bus. The power flow in the test system results in power losses of 210.5 kW, and the primary system voltage of 12.56 KV. This section displays the conventional IEEE 33-bus test network framework with a 3.72 MW active load and the reactive load of 2.3 MVAR, 5 ties, with 68 sectionalizing lines that divide buses. The numbers 1-68, and 69-73, correspondingly, are assigned to the tie lines. The RDN data are accessible in, [21], [24], [25]. Power losses occur as a result of the test system's 225 kW power flow, and the primary network voltage of 12.7 kV.

- First scenario: Considering the system loading of 80% with UPQC position whenever the parallel inverter supplies imaginary power needed for the load in an RDN without reconfiguring. In this scenario, the UPQC inverter operates in-dependently, with the shunt inverter bearing the whole load of the imaginary power need of the load for the duration of disturbances. In contrast, the series inverter delivers the real power required by the load during disturbances. This is accomplished using hybrid GA-IPSO for decision-making at the best location.
- Second scenario: Considering the system loading of 80% with UPQC position when the series and parallel inverters combined production of imaginary powers in RDN while reconfigured. Hence, the UPQC-recommended PAC is enabled. The I-UPQC series inverter is made to work with a shunt inverter to share load-imaginary power while simultaneously reducing voltage dip/swell. The imagi-nary load power-sharing between the two inverters was structured using the PAC control technique, and the voltage dip/swell was reduced using the real power control approach. This is accomplished by the application of hybrid GA-IPSO for decision-making at the best location.
- Third scenario: a continuous condition of 80 % loading considering the series and parallel inverter with the influence of PAC interlinked and DG in an RDN is accomplished for PQ without reconfiguration. In order to make decisions in the best place on the network, hybrid GA-IPSO is used. Through a shunt inverter, the PV is incorporated and plugged by real power injection into the load in the event of a dip. In a similar vein, the I-UPQC kept the initial procedure going while increasing the quantity of imaginary power delivered by the VSI connected in series and lowering t UPQC's magnitude for a specific level of dip/surge. By utilizing a hybrid of GA-IPSO for decision-making, this is accomplished through the optimal location.

4 Simulation and Results

The investigation simulations and findings from two RDN are presented in this part. In this study, the 33-bus and 67-bus were employed separately along with the I-UPQC model. All simulation iterations were run using the certified test RDN data from, [22], [23], [26], with balance loading as a baseline. The only swing bus shared by the two networks was at the substation, and the other bus were load (Q) buses. The slack bus voltage was given as 1,0 p.u. per unit. Three examine UPQC modes were tested under methodologies scenario on three distinct ratios of the highest voltage produced from the VSI's output to the projected load voltage K_{Sinj}, 20 %, 39.9 %, and 59.9 % in connection to dip/surge.

4.1 Utilizing Convergence Evaluation to Assess PQ in 33-bus Systems without/with PAC

This section presents 60 % of the study of GA-IPSO convergence centered on the best UPQC allocation in the RDN compared to the other simulations in three test scenarios. Figure 4 depicts the convergence investigation with GA-IPSO and RDN, which considers most cases at 60% disruption. The convergence provides the best spot for the I-UPQC's inverters to effectively share imaginary power. The test system's ability to improve reactive power is also shown in Figure 4 as a result of a 60 % injection. It is noted that the chosen approach gives convergence of 0.151 in second scenario and 0.156 in first scenario at 59.9 % provided, during the 40th iteration, case 3 converges at 0.148. This section illustrates the distribution system for three sites compared to other models.

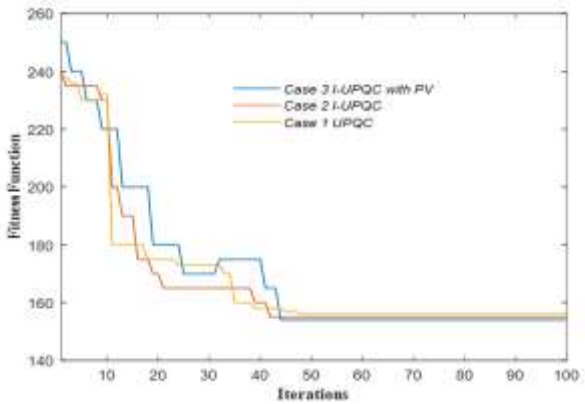

Fig. 4: Analysis of convergence on 33-bus at a single I-UPQC location with a 60 % injection

Figure 5 shows the convergent study of the network for the best placements at 40% injection. Also, Figure 5 displays a more accurate convergence assessment provided by GA-IPSO on the network for the whole assessment cases at 39.9 % penetration for the period of disruption. The FF is lowered in this case to allow for an increase in iterations, and it converges at its global minimum. As demonstrated in Figure 4, because of the 40 % injection, the network under test's FF ability also met the imaginary power amelioration distinct requirement. In other to fulfill the need for the loads during sag and swell, the series inverter injects extra imaginary at bus 6 of the network. The selected strategy is seen to produce convergence when case 3 converges at 0.148 at iteration 48, case 2 at 0.150 at iteration 44, and case 1 at 0.155 for 40 % injection.

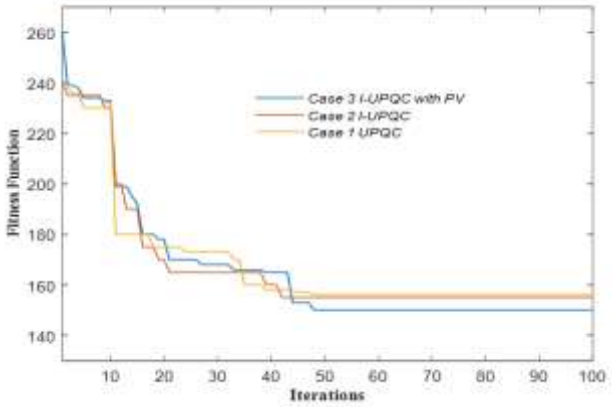

Fig. 5: Analysis of convergence on 33-bus at a single I-UPQC location with a 40 % injection

The assessment in Figure 6 shows the results of the system convergence study for the best placements at a 20 % injection. The more accurate convergence analysis provided by GA-IPSO is displayed in Figure 6 on the system for all test cases at 20 % of injection during the disruption period. In this case, the FF is reduced to boost the repetition amount and comes together at a global minimum. Due to a 20 % injection, the test system FF also met the requirements for imaginary power amelioration, as illustrated in Figure 6. The series inverter is located at network bus 6.

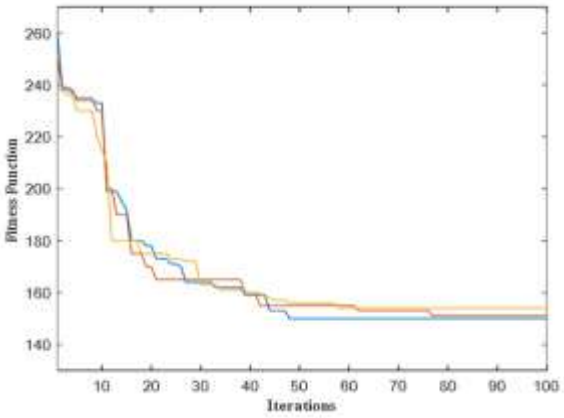

Fig. 6: Analysis of convergence on 33 buses at a single I-UPQC location with a 20 % injection

4.2 Evaluation of PQ Convergence on 69-bus RDN with/without PAC

This section compares the GA-IPSO and UPQC best allocation in the RDN to the other models for the three test scenarios. Figure 7 shows the convergence study of the GA-IPSO in the RDN for the whole assessment cases of 59.9 % of injection for the duration of the disruption. The convergence provides the best site for the series and shunt inverters to efficiently share imaginary power. Similar to Figure 7, the test system FF for imaginary power amelioration is evident due to 60% injection. It should be noted that the selected approach yields convergence of 0.1352 for second scenario and 0.147 for the first scenario of 60 % provided in RDN over other models for three positions shown in this segment. Case 3 converges at 0.139 at the 49th iteration.

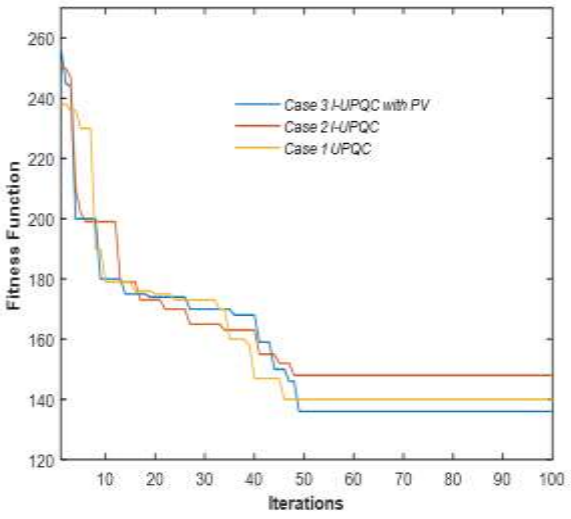

Fig. 7: Analysis convergence on 69 buses at a single I-UPQC location with a 60 % injection

The illustration in Figure 8 depicts the results of the convergence analysis of the network for the optimal places at a 40 % injection. Also, Figure 8 displays a superior convergence evaluation provided by GA-IPSO on the network for the whole assessment scenario of 39.9 % of injection for the period of disruption. The FF is reduced in this case to raise the number of repetitions that converge at the global minimum. Imaginary power compensation, which is evident as illustrated in Figure 6 because of a 40% injection, was also met by the test system FF. In order to fulfill the need for the loads during sag and swell, the series inverter injects extra reactive at bus 6 of the network. The adopted strategy is seen to produce convergence at iteration 49th when case 3 converges at 0.148. At iteration 44, case 2 converges at 0.146, and at iteration 46, when case 1 at 40% injection converges at 0.146.

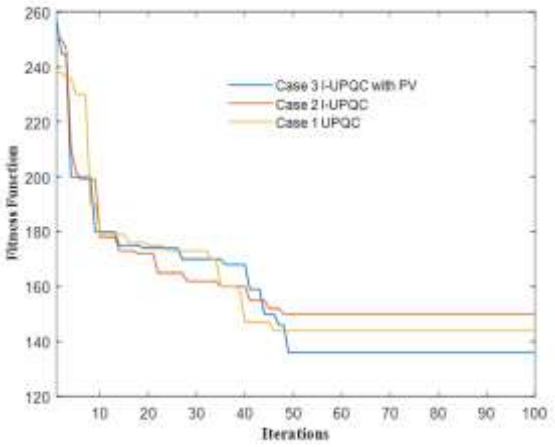

Fig. 8: Analysis convergence on 69 buses at a single I-UPQC location with a 40 % injection

In Figure 9, the convergence study of the system is shown for the best spots at a 20 % injection. Likewise, in Figure 9 presents a more accurate convergence analysis that GA-IPSO provides on the network for all test cases at a 25% injection rate for the period of disruption. Here, the FF is constrained to converge at the global minimum after an increase in the number of iterations. Similar to how the 25% injection met the network under consideration FF, the reactive power mitigation evidence is presented in Figure 9. The series inverter injects extra reactive at bus 6 of the network to fulfill the demand from the loads at the occurrence of sag and swell. The accepted strategy is seen to give convergence when case 3 converges at 0.138 at iteration 60, case 2 at 0.139 at iteration 44, and case 1 at 0.143 at 25 percent addition. Hence, a global minimum convergence was indicated from the above

repetition evaluation for GA-IPSO at 25% superior to 40%, and 60% K_{Sinj}.

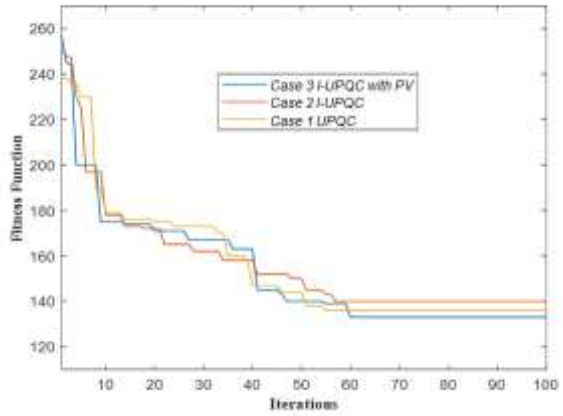

Fig. 9: Analysis convergence on 69 buses at a single I-UPQC location with a 20% injection

5 The VA Size of I-UPQC Installed on Every Bus

As shown in Figure 10 (a) and Figure (b), in that order, the VA capability of I-UPQC when it is situated correctly in 33 and 69 bus RDN. The VA rating of the device installed in the ideal position consistently demonstrates an improvement above the results obtained using an analytical technique at each network bus. Employing GA-IPSO, it was determined that the busses 17 and 61 of the networks were the optimum locations for PQ enhancement in terms of sharing imaginary power amid voltage dip, surge, and the decrease of power loss. This is a substantial improvement above the requirement for the high I-UPQC's capability that is positioned closer to the substation. The GA-IPSO integrated the requirement for reactive power sharing with the predicted greater load current coupled with a substantial load. Therefore, in these circumstances, more reactive power amelioration is required. However, Figure 10 (a) and Figure (b) show the quantity of VA distributed by VSI linked in series at different points in the two RDN. Given a spike in the size of series injected voltage, the Figures show that VSI linked in series gives better amelioration.

As seen in Figure 10(a) shows that case 1 and case 2 have minimum capacities of 0.1 kVA and 0.070 kVA, respectively, due to imaginary capacity sharing and ideal positioning at bus 17, whereas case 3 has the lowest capacity on the network, with I-UPQCpv showing a VA capacity of 0.02 kVA. It is also observed that Case 3 still has a lower VA rating despite the DG interconnection, and even with a 25% dip/surge, the series inverter still provides imaginary power amelioration. The situation is the same for the 69-bus network as well. For cases 3, 2, and 1, 0.50 kVA, 0.70 kVA, and 0.90 kVA of capacity have been attained. In line with the findings, I-UPQC installed in RDN with a PAC monitored inverter reduced its capability in bus 61, and in the third scenario, while the VSI linked in parallel was connected to PV, it further reduced the rating to a very low level.

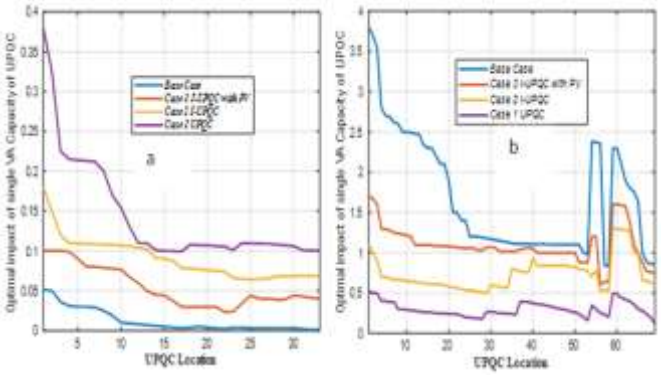

Fig. 10: I-UPQC assignment on buses 33 and 69, respectively

5.1 Effect of Optimal I-UPQC Allocation on RDN Loss Minimization

The examples in Figure 11 (a) and Figure (b) show the appropriate I-UPQC distribution at every node in the two systems and the energy losses in the bus. Prior to I-UPQC assignment, the losses generated at buses 33 and 69 are 202.67 and 224.98 kW, correspondingly. The outcomes show that nodes 61 and 17 in the 69 and 33 networks system of RDN, which are the locations where the largest amount of Loss Reduction (LR) was accomplished, were equipped with I-UPQC. To acquire the best imaginary power amelioration, these are the possible positions for the test systems. The I-UPQC assignment causes a drop in the network's peak line current. The highest line current measured in both systems without using I-UPQC amount to 0.0382 and 0.0391 per unit. For examples 2, and 3, an actual drop in the highest line current also reduced power loss. At various levels of K_{Sinj}, however, given that the overall imaginary power improvement is proportionate to the imaginary load power requirements, which is consistent, there were no noticeable changes. A similar occurrence happened in case 3, where the least power dissipated was observed at 33-bus and 69-bus, individually, accounting for 128 kW and 124 kW, which together accounted for 60 % of the total power loss. In test RDN, bus 5 and bus 61 for 33-bus and 69-bus were

the candidate buses where the least power loss was observed owing to the I-UPQC connection.

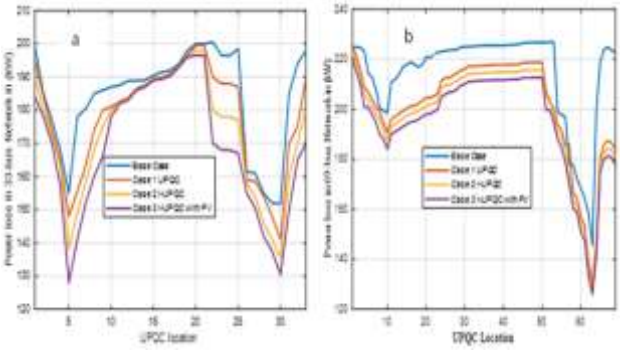

Fig. 11: I-UPQC Assignment in Network Test System of buses 69 and 33 cause power loss

5.2 Impact of Optimal I-UPQC's Placement on Preventing Low Voltage

In I-UPQC, the shunt and series VSIs shared imaginary power, which helped to reduce under-voltage in terms of controlling imaginary power. The amount of Low Voltage Compensation (LVC) on bus was used to calculate the influence of I-UPQC on RDN voltage. Figure 12 (a) and Figure (b) illustrate this. The placement of I-UPQC at the RDN network', ideal bus, as shown by the K_{Sinj}, revealed the same proportion of LVC at the same nodes. In the case of the 69 buses, nine buses, or around 12.9% of them, where sags issues are noted without I-UPQC placement, making up around 24 out of the 33 buses, or about 63.63 %. The nodes 17 of 33-bus and 61 of 69-bus systems perform better in the ideal I-UPQC position for dip-voltage mitigation, with the highest sag-voltage mitigation of 72 percent and 75 percent, respectively, respectively, in both systems at case 3. Additionally, I-UPQC, which was best positioned at bus 17 in the 33-bus network, gave the best under-voltage prevention in all K_{Sinj} cases, whereas bus 61 in the 69-bus system got results for K_{Sinj} cases. According to the LVC analysis, case 3 showed a higher proportion of energy generated thanks to the coupling of the PV to the shunt inverter. In the same way, example 2 shows a 65 and 70 % voltage dip mitigation, compared to 60 and 65 % in case 1. As a result, it can be determined that example 3 exhibited a superior LVC in Figure 12.

The series VSI can be employed in I-UPQC at its ideal position for VA capacity reduction, voltage dip amelioration, and imaginary power adjustment. As a result of an increase in K_{Sinj}, VSI linked in series supplied more amelioration. If I-UPQC is assigned at a specific location inside the RDN, substantial enhancements in VP, the power dissipated, and imaginary power distribution can be made. The lowest bus voltage from the 33-bus and 69-bus is seen from the simulation model to be 0.9979 p.u., and 0.9931 p.u., correspondingly, by the placement of I-UPQC among all unique load buses with many iterations.

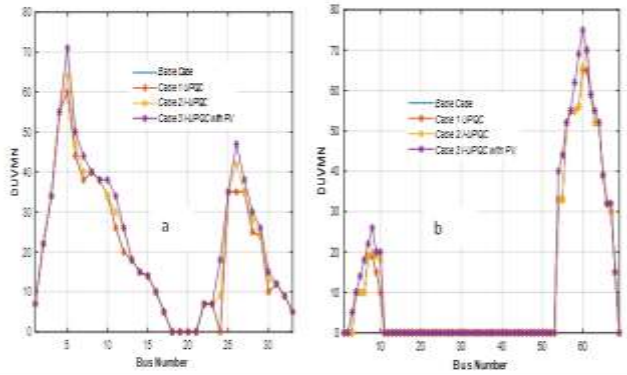

Fig. 12: UVMN effect predicated on I-UPQC deployment at the specific bus

The candidate bus provides the best imaginary power amelioration. It was also observed that an increase in K_{Sinj} had no effect on any of the metrics considered in this study, including voltage profile and power loss. The findings revealed that the chosen candidate bus, which are nodes with a heavy load, is where I-UPQC is acquired when a site satisfies the criterion. In the meantime, The nodes 68 and 18 of the test system 69 and 33 RDN, respectively, appeared to be the best places for hypothetical power distribution and sharing for reducing voltage dip/surge in Cases 2 and 3 at a 25% disturbance in the system, respectively. Because the quantity of active power needed is so little and the shunt inverter readily injects the necessary amount of active, it appears that several buses in both the 33 and 69 bus in Case 3 did not absorb real power through the series inverter. That is to say, there is zero active power injection in those that are being monitored.

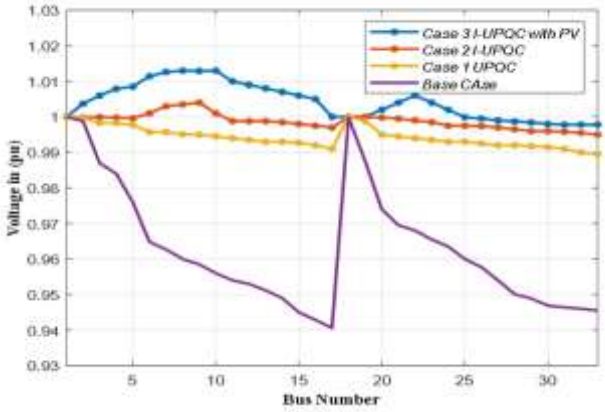

Fig. 13: 33-bus test voltage profile at a 25% injection

5.3 Voltage Profile at 20% in 33 and 69 RDN with and without PAC

Figure 13 compares the voltages in cases with and without a UPQC PAC as well as PV connections with UPQC under PAC control. As presented in Table 1, the level of voltage increased to 0.9901 from 0.9463 per unit at node 18 for standard UPQC, as compared I-UPQCPV while considering node 18, which increase to 0.9988 from 0.9979 per unit. Additionally, Figure 14 below provides the outcome for 69-bus for comparing the situation with and without a PAC of UPQC, followed by the connectivity of PV under PAC management. As shown in Table 2, the voltage level with UPQC increased to 0.9730 from 0.9203 at node 68, while I-UPQCPV increased to 0.9920 from 0.9890 per unit at the same node. When the new device was linked to the analytical placement through a single VSI connected in parallel integration, the I-UPQC efficiency shows that the VP was thus enhanced further. Thus, the success of I-UPQC instance 3 at disruption of 25% indicates that the inverter series provided extra imaginary power, producing a stronger VP in comparison to a disruption of 39.9 % and 59.9 %. The quantity of imaginary power generated in the first and second scenarios at a 20 % disruption also cancels out first scenario quantity, placing an imaginary power liability on the shunt inverter in those cases. The case 3 design with better VP also yields the position relating to minimum power dissipation at node 18 for a 33-bus system and node 68 for a 69-bus network.

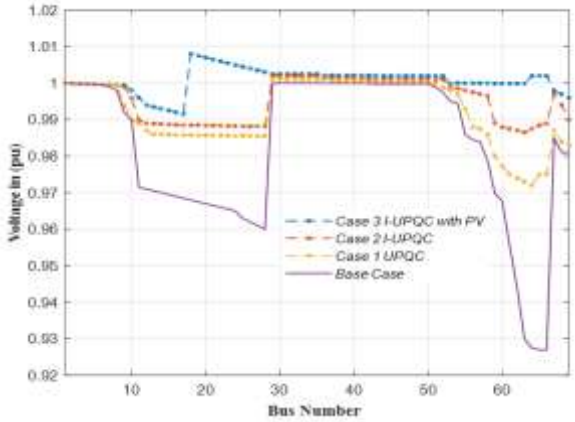

Fig. 14: The 69-bus RDN voltage profile at 20% injection

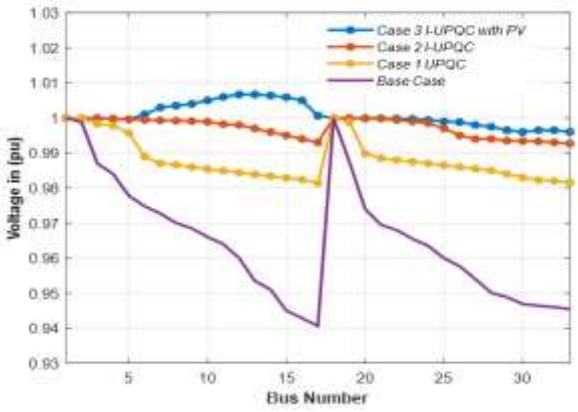

Fig. 15: At 40% injection, the VP of the 33-bus RDN

5.4 Voltage Profile at 40 % in 33 and 69 RDN with and without PAC

The comparison of voltage for the cases with and without a UPQC PAC is shown in Figure 15 and Figure 16, followed by the case with PV connections under PAC control. According to Table 1 and Table 2, the level of voltage increased to 0.9810 from 0.9363 per unit at node 18 for standard UPQC, as compared I-UPQC while considering the same node, which increase to 0.9981 from 0.9900 per unit for I-UPQCPV. A PAC with UPQC was used in the case with and without the connection of PV under PAC control, and the results for 69-bus are shown in Figure 16. As indicated in Table 2, with regular UPQC, the voltage level increased to 0.9710 from 0.9303 per unit at node 17, while I-UPQC increased to 0.9810 and I-UPQCPV to 0.9730 per unit at the same node. The entire I-UPQC results show that the VP enhanced more when the new device was coupled through the VSI connected in parallel at a single integration with the analytical positioning. A better VP than 60 % disruption but less than 20 % disruption VP alleviation was achieved because of the execution of I-UPQC case 3 at a 40 % disturbance. Similar to how case 1 places an imaginary load on the shunt inverter, the second scenario imaginary power injection is improved as compared to the first scenario but significantly lower in third scenario.

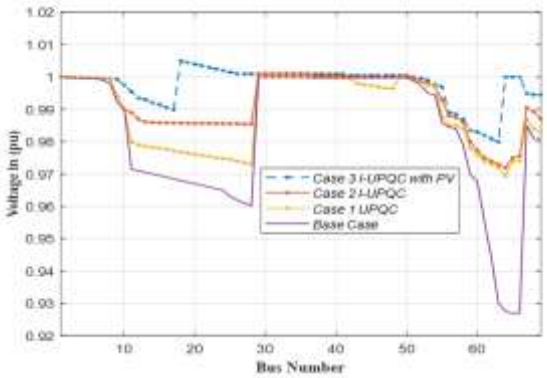

Fig. 16: At 40% injection, the VP of the 69-bus test system

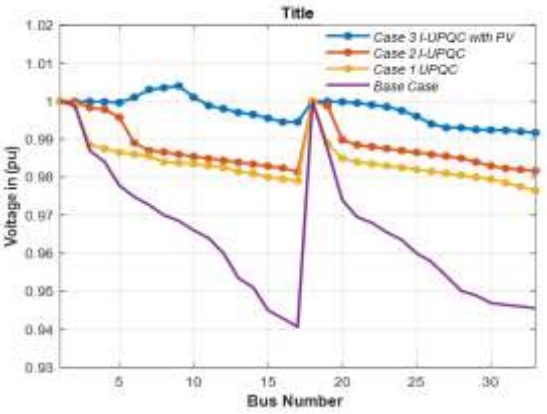

Fig. 17: At 60% injection, the VP of the 33-bus test system

5.5 Voltage Profile at 60% in 33 and 69 RDN with/without PAC

The voltage evaluation for cases with/without a PAC of UPQC and for the case of PV connection with UPQC and PAC control is shown in Figure 17 and Figure 18. The voltage on bus 18 was increased to 0.9780 from 0.9453 p.u when standard UPQC is used and 0.9850 p.a. when I-UPQC is used on buses 18 and Figure 19, respectively, as shown in Table 1. Figure 18 shows the results for 69 test systems in order to compare the scenario with/without PAC installation to UPQC, with the influence of PAC and PV connection. As shown in Table 1, the voltage level increased to 0.9599 to 0.9303 per unit at node 68 for regular UPQC, while with I-UPQC, it increased to 0.9720, and with I-UPQCPV to 0.9705 per unit at the same 68 node. According to the overall I-UPQC function, the VP enhanced more when the latest device was linked to the VSI coupled in parallel at a single integration with the optimal location. The overall I-UPQC result proves the VP enhanced more when the new device was linked single connection with the analytical positioning through the shunt inverter. But when the I-UPQC was linked to the PV across the VSI connected in parallel, the results were even better.

6 Comparison of Findings

Subsequently, the aforesaid findings, a comprehensive and accurate examination of the effects of I-UPQC in taking into account VP enhancement and loss minimization by correlating the base case, first, second and third scenarios become necessary. Though, UPQC, I-UPQC, and I-UPQCPV are crucial points of evaluation in Figure 19 and Figure 19, Table 1 and Table 2 provide a summary of this influence for both 33-bus and 69-bus. Figure 18 and Figure 19 depict the hypothetical power distribution between the two inverters in series and shunt configuration in a similar manner.

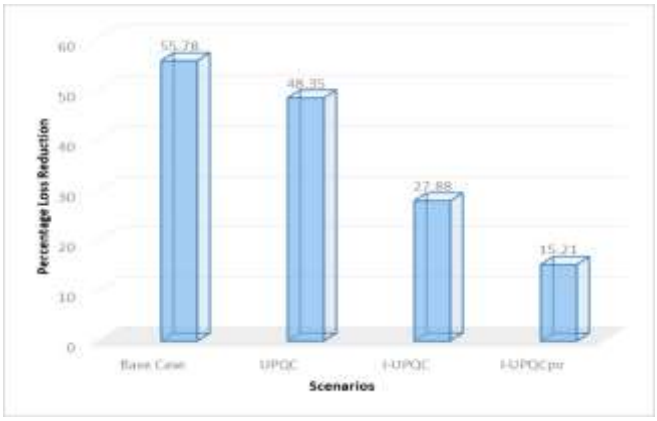

Fig. 18: Power dissipation of 33-bus RDN in all cases

6.1 Comparison of Power Dissipated in the 33-bus with the best I-UPQC Allocation

As indicated in Table 1, the impact of I-UPQC outcomes over conventional UPQC with-out PAC are compared in 33-bus RDN overall. The I-UPQC demonstrates that bus 6 of 33-bus has a series inverter that provides extra imaginary power in PAC-controlled models. When examining the outcomes from various scenarios, it is found that a 25% disturbance in RDN with I-UPQC gives greater power dissipation minimization. Because of the ability of the parallel inverter to supply the real power demanded by the load in the occurrence of a dip and absorbed imaginary power in the event of a surge, the network connected to PV via I-UPQC exhibits a greater decrease in comparison. Figure 19 depicts the percentage power loss decrease in each example, and I-UPQC was found to have the lowest proportion of 15.21 %. According to the findings, case 3 PV connections through the shunt inverter

can significantly reduce loss if it is properly constructed and regulated at the proper position.

Table 1. Comparing the I-UPQC model to the standard UPQC in the 33-test system

Scenarios	UPQC Position	Name	Peak load
Base Case	No UPQC	Lowest VP (p.u.)	0.9463
		Dissipated Power (kW)	51.59
		Lowest VSI	0.8369
First scenario: UPQC	Bus 18	Lowest VP (p.u.)	0.9900
		Dissipated Power (kW)	23.55
		% LR (kW)	48.35
		Lowest VSI	0.9041
		Shunt injected (kVar)	0.202
Second scenario: I-UPQC	Bus 18	Lowest VP (p.u.)	0.9969
		Dissipated Power (kW)	35.14
		% Loss Decrease (kW)	27.88
		Lowest VSI	0.9053
		Series injected (kVar)	0.090
		Shunt injected (kVar)	0.112
Third scenario: I-UPQC with PV	Bus 18	Lowest VP (p.u.)	0.9989
		Dissipated Power (kW)	14.79
		% LR (kW)	15.21
		Lowest VSI	0.9362
		Series injected (kVar)	0.1050
		Shunt injected (kVar)	0.0987

6.2 Comparison of 33-bus Imaginary Power Sharing in Cases with and without PAC

Figure 19 illustrates the injection of imaginary power between the two inverters in the 33-bus RDN for the period of imaginary power improvement in the case of dip reduction at 25%. According to the UPQC in the RDN, case 1, a complete imaginary load was carried by the shunt inverter and was 0.202 kVar, whereas the series provided all real power. However, whereas the shunt inverter injects 0.101 kVar, the series inverter only supplies 0.051 kVar. Case 3 ultimately performs better due to its involvement in imaginary power amelioration during the disruption when the I-UPQC device is triggered. In the condition of integrated PV through the shunt inverter, the series VSI provides 0.1499 kVar, and the parallel VSI produces 0.1011 kVar in node 6. Due to PAC control, it has been indicated that I-UPQC outperforms in terms of imaginary power improvement.

Fig. 19: Imaginary power amelioration for parallel/series inverters in 33-test system

6.3 Evaluation of Power Dissipation on 69-Test System RDN with/without PAC

Table 2 shows the total evaluation of the effect of I-UPQC findings above regular UPQC without PAC in three scenarios for the 69-test system RDN. At node 61 of 69 test system, the I-UPQC demonstrates that series inverters provided so much imaginary power in PAC regulated models. Under a disturbance of 25%, it is found that radial networks with I-UPQC offer a greater decrease in power loss when comparing the findings from various scenarios. The network connected to PV through I-UPQC exhibits a higher decrease in comparison due to the parallel inverter's ability to provide the real power that the consumer needs in the occurrence of undervoltage and absorbed imaginary power in the event of a surge. In the 69-test system, I-UPQC had the lowest percentage, or 18.50%, where the proportion of power dissipation minimization for each example is shown in Figure 20. According to the findings in case 3, PV connections through the shunt inverter can significantly reduce loss if it is properly constructed and regulated at the right position.

Fig. 20: Loss of power in all 69-bus network test instances

Table 2. Comparing the I-UPQC model to the standard UPQC in the 69-test system

Scenarios	UPQC Position	Name	Peak load
Base Case	No UPQC	Lowest VP per unit	0.9203
		Dissipated Power (kW)	51.59
		Lowest VSI	0.8369
First scenario: UPQC	Bus 68	Lowest VP per unit	0.9720
		Dissipated Power (kW)	23.55
		% LR (kW)	40.35
		Lowest VSI	0.9041
		Shunt injected (kVar)	0.269
Second scenario: I-UPQC	Bus 68	Lowest VP per unit	0.9870
		Dissipated Power (kW)	35.14
		% LR (kW)	27.4
		Lowest VSI	0.9053
		Size of UPQC in (kVar)	0.61
		Series injected (kVar)	0.133
		Shunt injected (kVar)	0.126
Third scenario: I-UPQC with PV	Bus 68	Lowest VP per unit	0.9930
		Dissipated Power (kW)	14.79
		% LR (kW)	18.5
		Lowest VSI	0.9362
		Size of UPQC in (kVar)	0.41
		Series injected (kVar)	0.149
		Shunt injected (kVar)	0.131

6.4 Comparison of 69-bus Imaginary Power Sharing with and without PAC

Figure 21 shows how the two inverters in the 69-test system RDN share imaginary power when in an imagined power improvement in the case of dip reduction at 24.9%. The shunt inverter assumed the responsibility for all imaginary power in scenario 1 of 0.269 kVar, according to the UPQC in the RDN. Hence, the series provided most of the real power. However, the shunt inverter only injects 67.5 reactive power, whereas the series inverter produces 84.5 reactive power. Case 3 ultimately performs better by taking part in imaginary power amelioration during the disruption when I-UPQC was in use. When connected PV via the parallel inverter, the series inverter offers 183.6 reactive power, whereas the parallel inverter gives 135.6 reactive power on the node 6. It has been demonstrated that I-UPQC outperforms PAC in aspects of compensating for imaginary power.

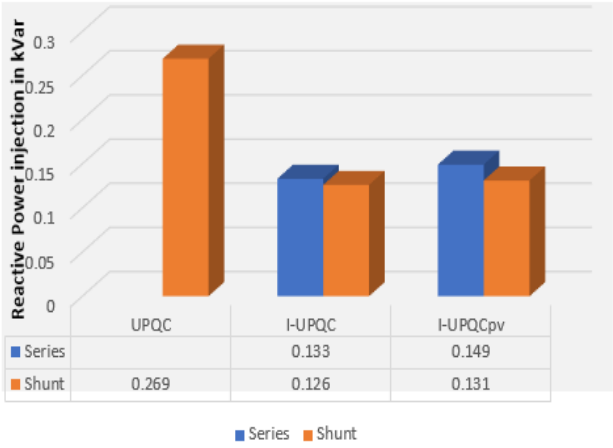

Fig. 21: Compensation of imaginary power in 69-test system among both parallel/series inverter

7 Conclusion

A specific quantity of under-voltage in the RDN was effectively reduced by using a spe-cial PAC of the UPQC configuration known as I-UPQC. For the study, the I-UPQC model was best included using a load-flow method with GA-IPSO. The results of this investigation led to the following conclusion. I-UPQC located at an optimal node can reduce VA capacity while reducing imaginary power consumption. I-UPQC installed at a particular RDN node significantly reduces power loss. Additionally, certain nodes achieve better VP enhancement at sending and receiving end of the RDN. However, the results show that a candidate bus must be situated optimally with a greater capacity I-UPQC to perform at its best. As a result, the performance of I-UPQC in RDN depends on the position. It also demonstrates higher power reduction with an ideal method than analytical placements and improves under-voltage. The voltage sags, VP variations, and actual power loss of the tested systems were all adequately managed with the help of the research methods and outcomes. It is evident that I-UPQC showcases the proper sharing of imaginary power while optimal placement enhances its operation in RDN. The outcomes showed that, at a preset degree of disturbance in a particular area, I-UPQC with a lower capacity could mitigate sag/swell. I-UPQC

coupled to PV using the same control strategy achieves a better improvement with active power absorbed via a parallel inverter. Although the assessment of optimal improvement strategy was effectively conducted, the dynamic behavior was not, and this can be a topic for more investigation.

References:

[1] D. Ćetković, G. Klobučar, and V. Komen, "Analysis of the Impact of Reactive Power Compensation on the Electric Power Quality of the LV Consumers in Distribution Networks of Various Characteristics," in 2022 45th Jubilee International Convention on Information, Communication and Electronic Technology (MIPRO), 2022, pp. 796–799.

[2] G. Chen, J. Zhang, and M. Taleb Ziabari, "Optimal allocation of capacitor banks in distribution systems using particle swarm optimization algorithm with time-varying acceleration coefficients in the presence of voltage-dependent loads," Aust. J. Electr. Electron. Eng., vol. 19, no. 1, pp. 87–100, 2022.

[3] O. O. Oluwole, "Optimal allocation of distributed generation for power loss reduction and voltage profile improvement," University of Cape Town, 2016.

[4] Y. Maataoui, H. Chekenbah, O. Boutfarjoute, and R. Lasri, "Voltage control using fuzzy logic for radial distribution network with high penetration of photovoltaic generators," in E3S Web of Conferences, 2022, vol. 351, p. 1030.

[5] H. Lotfi and A. A. Shojaei, "A dynamic model for multi-objective feeder reconfiguration in distribution network considering demand response program," Energy Syst., pp. 1–30, 2022.

[6] H. B. Tolabi, M. H. Ali, and M. Rizwan, "Simultaneous reconfiguration, optimal placement of DSTATCOM, and photovoltaic array in a distribution system based on fuzzy-ACO approach," IEEE Trans. Sustain. Energy, vol. 6, no. 1, pp. 210–218, 2014.

[7] A. Gupta, "Power quality evaluation of photovoltaic grid interfaced cascaded H-bridge nine-level multilevel inverter systems using D-STATCOM and UPQC," Energy, vol. 238, p. 121707, 2022.

[8] R. K. Chauhan, J. P. Pandey, and M. Hasan, "Comparative performance of the various control techniques to mitigate the power quality events using UPQC," in Advanced Computational and Communication Paradigms, Springer, 2018, pp. 31–40.

[9] P. K. Ray, P. S. Puhan, A. K. Das, D. Pradhan, and L. Meher, "Comparative Analysis of Different Control Techniques Implementation in UPQC for Power Quality Improvement," in Sustainable Energy and Technological Advancements, Springer, 2022, pp. 147–161.

[10] A. Patel, S. K. Yadav, and H. D. Mathur, "Utilizing UPQC-DG to export reactive power to grid with power angle control method," Electr. Power Syst. Res., vol. 209, p. 107944, 2022.

[11] O. O. Osaloni and A. K. Saha, "Voltage Dip/Swell Mitigation and Imaginary Power Compensation in Low Voltage Distribution Utilizing Improved Unified Power Quality Conditioner (I-UPQC)," in International Journal of Engineering Research in Africa, 2020, vol. 49, pp. 84–103.

[12] O. O. Osaloni and A. K. Saha, "Impact of Improved Unified Power Quality Conditioner Allocation in Radial Distribution Network," Int. J. Eng. Res. Africa, vol. 59, pp. 135–150, 2022.

[13] A. Patel, H. D. Mathur, and S. Bhanot, "Improving Performance of UPQC-DG for Compensation of Unbalanced Loads," in 2018 8th IEEE India International Conference on Power Electronics (IICPE), 2018, pp. 1–6.

[14] J. H. Yi, R. Cherkaoui, M. Paolone, D. Shchetinin, and K. Knezovic, "Optimal Co-Planning of ESSs and Line Reinforcement Considering the Dispatchability of Active Distribution Networks," IEEE Trans. Power Syst., 2022.

[15] A. Parizad, H. R. Baghaee, A. Yazdani, and G. B. Gharehpetian, "Optimal distribution systems reconfiguration for short circuit level reduction using PSO algorithm," in 2018 IEEE Power and Energy Conference at Illinois (PECI), 2018, pp. 1–6.

[16] P. Ramsami and R. T. F. A. King, "Multi-Objective Optimisation of Photovoltaic Systems and Unified Power Quality Conditioners with Simultaneous Distribution Network Reconfiguration," in 2020 3rd International Conference on Emerging Trends in Electrical, Electronic and Communications Engineering (ELECOM), 2020, pp. 191–197.

[17] T. Guan, F. Han, and H. Han, "A modified multi-objective particle swarm optimization based on levy flight and double-archive

mechanism," IEEE Access, vol. 7, pp. 183444–183467, 2019.

[18] O. Osaloni and K. Awodele, "Analytical Approach for Optimal Distributed Generation Allocation in Primary Distribution Networks," in Proc. 2016 South African Universities Power Engineering Conference, pp. 115–120.

[19] P. Jangir and I. N. Trivedi, "Non-dominated sorting moth flame optimizer: A novel multi-objective optimization algorithm for solving engineering design problems," Eng. Technol. Open Access J., vol. 2, no. 1, pp. 17–31, 2018.

[20] G. Carpinelli, F. Mottola, D. Proto, and A. Russo, "A Decision Theory Approach for the Multi-objective Optimal Allocation of Active Filters in Smart Grids," in 2022 20th International Conference on Harmonics \& Quality of Power (ICHQP), 2022, pp. 1–6.

[21] O. O. Osaloni, "Power quality improvement in low voltage distribution network utilizing improved unified power quality conditioner.," 2020.

[22] C. U. Eya, A. O. Salau, S. L. Braide, S. B. Goyal, V. A. Owoeye, and O. O. Osaloni, "Assessment of Total Harmonic Distortion in Buck-Boost DC-AC Converters using Triangular Wave and Saw-Tooth based Unipolar Modulation Schemes", WSEAS Transactions on Power Systems, vol. 17, pp. 324-338, 2022.

[23] O. O. Osaloni, A. S. Akinyemi, A. A. Adebiyi, A. O. Salau, "An Effective Control Technique to Implement an IUPQC Design for Sensitive Loads in a Hybrid Solar PV-Grid Connection", WSEAS Transactions on Power Systems, vol. 18, pp. 26-38, 2023.

[24] O. O. Osaloni, and A. K. Saha. "Distributed Generation Interconnection with Improved Unified Power Quality Conditioner for Power Quality Mitigation," 2020 International SAUPEC/RobMech/PRASA Conference, 1-6.

[25] H. Kassahun, A. O. Salau, O. O. Osaloni, and O. Olaluyi: "Power System Small Signal Stability Enhancement Using Fuzzy Based STATCOM," PRZEGLĄD ELEKTROTECHNICZNY 8, 27-32, 2023.

[26] O. O. Osaloni, A. S. AKINYEMI, A. A. Adebiyi, T. O. IBITOYE "Power Loss Analysis with Dispersed Generation in Multifunction Power Conditioner Design to Improve Power Quality" WSEAS Transactions on Power Systems, vol. 18, pp. 94-103, 2023.

Contribution of Individual Authors to the Creation of a Scientific Article (Ghostwriting Policy)

The authors equally contributed in the present research, at all stages from the formulation of the problem to the final findings and solution.

Sources of Funding for Research Presented in a Scientific Article or Scientific Article Itself

I want to use opportunity to appreciate Durban University of Technology and Afe Babalola University for the success of this research work.

Conflict of Interest

The authors have no conflicts of interest to declare.